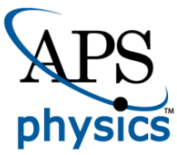

Role of finite-size effects in the critical behavior of itinerant fermions

Avraham Klein and Andrey Chubukov

Phys. Rev. B **96**, 041125 — Published 27 July 2017

DOI: 10.1103/PhysRevB.96.041125

Role of finite size effects in the critical behavior of itinerant fermions

Avraham Klein[1,*] and Andrey Chubukov[1]

[1] *School of Physics and Astronomy, University of Minnesota, Minneapolis. MN 55455*

We study the role of finite size effects on a metallic critical behavior near a $q = 0$ critical point and compare the results with the recent extensive quantum Monte-Carlo (QMC) study [Y. Schattner et al, PRX 6, 031028]. This study found several features in both bosonic and fermionic responses, in disagreement with the expected critical behavior with dynamical exponent $z = 3$. We show that finite size effects are particularly strong for $z = 3$ criticality and give rise to a behavior different from that of an infinite system, over a wide range of momenta and frequencies. We argue that by taking finite size effects into account, the QMC results can be explained within $z = 3$ theory.

Introduction Critical behavior in itinerant fermionic systems is a fascinating subject, which has attracted much interest in recent years, with particular emphasis on the behavior in two dimensions (2D)[1, 2]. Near a 2D quantum critical point (QCP), soft bosonic fluctuations of the order parameter field mediate strong interaction between low-energy fermions and destroy Fermi-liquid (FL) behavior down to a progressively small energy ω_{FL}, which vanishes at a QCP. Simultaneously, low-energy fermions affect soft bosonic fluctuations by (i) providing Landau damping and (ii) changing the bosonic mass. The destruction of the FL holds even if the overall strength of the interaction is much smaller than the fermionic bandwidth, i.e. when fermions remain itinerant throughout the transition.

Before the feedback from low-energy fermions is included, the inverse propagator of a soft boson is generally assumed to be an analytic function of momentum and frequency: $\chi^{-1}(\mathbf{q}, \Omega_m) \propto (|\mathbf{q} - \mathbf{Q}|^2 + \Omega_m^2/c^2)$, where $\mathbf{Q}$ is the momentum at which order parameter fluctuations condense at a QCP and Ω_m are Matsubara frequencies. The Landau damping comes from the insertion of the fermionic particle-hole bubble into the bosonic propagator. The form of the Landau damping term depends on whether $\mathbf{Q}$ has a finite value (e.g. (π, π) for a SDW QCP), or is zero, as for a nematic or a ferromagnetic QCP. In the first case the Landau damping term scales as just $|\Omega_m|$, while in the second case it scales as $|\Omega_m|/q$. In both cases, the Landau damping term wins at small Ω_m over the bare Ω_m^2 and changes the dynamical exponent from $z = 1$ to $z = 2$ for $Q \neq 0$ and to $z = 3$ for $Q = 0$. The one-loop fermionic self-energy due to scattering by Landau overdamped critical fluctuations has a non-FL frequency dependence in 2D: $\Sigma(\omega_m) \propto \omega_m^{1-1/z}$ ($\omega^{1/2}$ at particular hot spots along the Fermi surface (FS), when $Q \neq 0$, and $\omega^{2/3}$ everywhere on the FS, when $Q = 0$) [3–9].

For both $z = 2, 3$, higher order logarithmic singularities [7] likely cause a further flow of the critical exponents [10]. However, for $z = 3$ these corrections appear only at third-loop order [11–15] and should affect only the lowest frequencies (and possibly none [16]). In particular, one could expect the $z = 3$ behavior to be reproduced in numerical calculations, which probe the system at a finite T, when bosonic and fermionic Matsubara frequencies are discrete. It was quite surprising in this respect that the recent Quantum Monte Carlo (QMC) analysis of a model, designed to emulate a 2D nematic transition [17], found seemingly $z = 2$ behavior over a range of temperatures and frequencies. Furthermore, the same study found that the quasiparticle residue $Z = 1/(1 + d\Sigma/d\omega)$ remains finite down to the lowest frequencies when tuning across the critical point. Such disagreement with a basic, established theory is intriguing and should be understood.

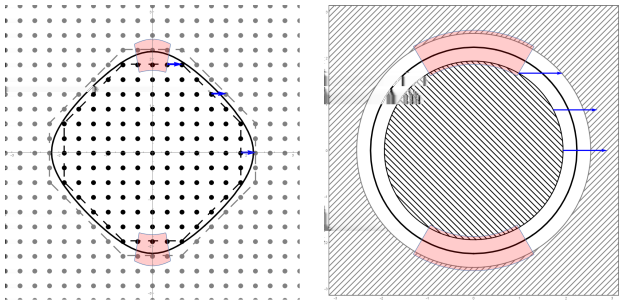

FIG. 1. (color online) Coupling of bosonic fluctuations and fermions in a finite system. The panel depicts the reciprocal space of a typical square lattice. The solid black line is the Fermi surface that would exist in an infinite system. Black (gray) dots are the filled (empty) states in $\mathbf{k}$-space. A bosonic fluctuation of wavevector $\mathbf{q}$ (blue arrows) can couple to fermions by exciting an electron-hole pair. In an infinite system, this coupling can occur at any point on the Fermi surface. However, in a finite system, the filled (empty) states actually appear as a series of terraces (dashed lines). As a result, for small enough q there is a region of the Fermi surface where excitations cannot occur (shaded region). The right panel depicts an approximation to the left panel, replacing the lattice with the electron/hole continuum with a gap in momentum space with the width $q_1 = \pi/L$, as described in Eqs. (7) and (8).

Several known mechanisms can make it difficult to extract $|\Omega|/q$ behavior from the data on $\chi(q, \Omega)$. First, when fermionic residue is small, $|\Omega|/q$ scaling is observed only when $v_F q > \Omega_m/Z$, a more severe restriction than

just $v_F q > \Omega_m$ [18]. Second, because the nematic order is not a conserved quantity, the bosonic propagator in 2D has an additional $q-$independent $\Omega^{2/3}$ term [19]. This term does not break $z = 3$ scaling but can mask $|\Omega|/q$ behavior. The form of the bosonic propagator is further complicated at finite T because of special contributions from thermal fluctuations, which act much like impurities [20, 21]. Third, if critical bosons are separate degrees of freedom, rather than collective modes of fermions, they may have their own damping in addition to Landau damping, and that damping doesn't have to have Ω/q form. These mechanisms, particularly the last one, were essential to understand the violation of Ω/q scaling in uranium-based itinerant ferromagnets UGe_2 and UCoGe [22–24]. They are, however, less relevant to QMC analysis because in this analysis intrinsic dynamics of bosons (fluctuations of localized spins of the transferred Ising model) can be separated from the effects due to fermions by switching on and off the coupling between the two degrees of freedom.

In this work we explore an additional, hitherto undiscussed aspect of the problem – a strong sensitivity of an itinerant QC system to finite-size effects. Landau damping is the source of this sensitivity. Bosonic fluctuations transfer energy most efficiently to electron-hole pairs with momenta parallel to the Fermi surface, i.e. when $\mathbf{q} \cdot \mathbf{k}_F \simeq 0$, where $\mathbf{q}$ is the bosonic momentum and$\mathbf{k}_F$ is on the Fermi surface. This fact is behind the well-known "patch" approximations in long-wavelength QC systems. In a finite system, discreteness of the Brillouin zone inhibits momentum transfer to the fermions, and does so most strongly precisely where the damping is strongest. See Fig. 1 for a graphical representation. The result is to introduce a new scale for damping. We show that in a finite system of size L, the polarization bubble, whose dynamical part yields the Landau damping at $L \to \infty$, is

$$\Pi(q, \Omega_m) = \Pi(\alpha, \beta), \ \alpha = \frac{|\Omega_m|}{v_F q}, \ \beta = \frac{q_1}{q}, \qquad q_1 = \pi/L. \tag{1}$$

Here, $\Pi(\alpha, \beta \to 0) = \gamma(1 - \alpha/\sqrt{1+\alpha^2})$ as for the infinite system. At a non-zero β, the form of $\Pi(\alpha, \beta)$ is determined by a combination of two effects: (i) $\Pi(0, \beta)$ decreases with increasing β ($\Pi(\alpha, \beta)$ vanishes at $\beta = 1$, see below), and (ii) $\Pi(\alpha, \beta)$ vanishes at $\alpha \to \infty$ for any β. As a result, there appears an intermediate range of $\alpha < 1$, where the variation of $\Pi(\alpha, \beta)$ vs α (i.e., vs $|\Omega_m|$) is roughly linear, but the slope decreases as β increases and over a rather wide range of parameters appears almost independent of q (see Fig. 2a). This mimics $z = 2$ scaling as reported in [17] (Fig. 2b). We also found that the data from Ref. [17] can be reproduced in an alternative, semi-phenomenological approach, by invoking the fact that in a finite system the polarization bubble vanishes not at $q = 0$, but at at $q = q_1$, i.e. at $\beta = 1$. Near $\beta = 1$, $\Pi(\alpha, \beta) \propto (1 - \beta)^{3/2}$ (see below). Assuming phenomenologically that this is the main finite-size effect, we approximate the frequency dependence of the polarization bubble as

$$\Pi(\alpha, \beta) = \Pi(\alpha, 0)(1-\beta)^{3/2} = \gamma \left(1 - \frac{\alpha}{\sqrt{1+\alpha^2}}\right)(1-\beta)^{3/2}. \tag{2}$$

This simple form reproduces the data from [17] to surprisingly good accuracy (see Fig. 2c).

The fermionic self-energy also has strong finite-size dependence. We found (for $\omega_m > 0$)

$$\Sigma(\omega_m) \propto \omega_1^{2/3} \left[\left(1 + \frac{\omega_m}{\omega_1}\right)^{2/3} - 1 \right] \tag{3}$$

where $\omega_1 \sim v_F q_1$ up to logarithms (see Eq. (14) below). At $\omega \gg \omega_1$ this yields $\Sigma(\omega_m) \propto \omega^{2/3}$, as in the infinite system. However, at smaller ω, $\Sigma(\omega_m) = a\omega_m + b\omega_m^2 + ...$ as in a FL. As a result, for probes at $\omega \geq \omega_1$, it looks as if the quasiparticle residue remains finite throughout the transition. We compared Eq. (3) with Ref. [17] and again found good agreement with QMC data (see Fig. 3).

Model calculations We consider a 2D system of size $L \times L$. The system is composed of electrons hopping on a lattice and coupled to a scalar boson field. The free propagators of electrons and bosons are of the form,

$$G^{-1}(\mathbf{k}, i\omega) = i\omega - \varepsilon_{\mathbf{k}}, \tag{4}$$

$$\chi^{-1}(\mathbf{q}, i\Omega) = \chi_0^{-1}(m^2 + q^2 + \Omega^2/c^2), \tag{5}$$

where c is the bosonic velocity, and $m = 1/\xi$ goes to zero at the QCP. In a finite system the interaction can be written as

$$H_I = -g \sum_{\mathbf{q},\mathbf{k}} f_{\mathbf{k}} \phi_{\mathbf{q}} \psi^\dagger_{\mathbf{k}+\frac{\mathbf{q}}{2}} \psi_{\mathbf{k}-\frac{\mathbf{q}}{2}}, \tag{6}$$

where $f_{\mathbf{k}}$ is a form factor, the $\mathbf{q}, \mathbf{k}$ sums are over the 1st bosonic and fermionic BZ's respectively, and g is a coupling constant. Let us recall the origin of the form $\Omega/v_F q$ for the polarization. It arises from the fact that for small enough $\Omega \ll v_F|\mathbf{q}|$ there is *always* an electron-hole pair that can be resonantly excited, given by the condition $\Omega = \mathbf{v_F} \cdot \mathbf{q} = v_F q \cos\theta$, as long as the FS is closed. However, as Eq. (7) shows, in a finite system and for small enough $\mathbf{q}$ it is not always possible to find such a pair. The reason for this is that in a finite system the border between filled and empty states is not a smooth curve but a series of "terraces" (Fig. 1). At small enough momentum and frequency it is no longer possible to find a resonant pair that also conserves momentum. This gives a lower cutoff of $\Omega < v_F q \sim v_F q_1$ for the overdamped behavior of the bosonic excitations, which introduces the new scale $\beta = q_1/q$, leading to Eq. (1). As long as $1 - \beta$ is not too small, the main effect of the discrete

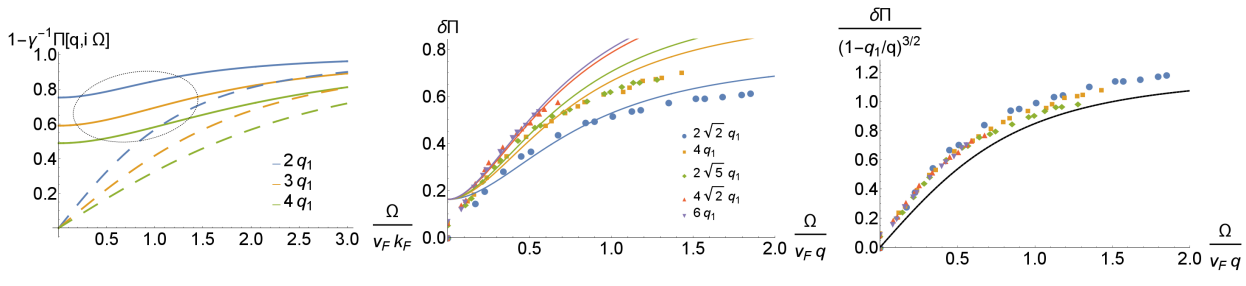

(a) (b) (c)

FIG. 2. (color online) Dynamic polarization bubble $\Pi(q,\Omega_m)$. In an infinite system, $\Pi(q,\Omega_m)=\gamma(1-|\Omega_m|/\sqrt{(v_Fq)^2+\Omega_m^2})$, i.e., the slope of $1-\Pi(q,\Omega_m)/\gamma$ scales as $1/q$. In a finite system, this behavior is modified because $\Pi(q,\Omega_m)$ vanishes at $q_1=\pi/L$. Panel (a) shows $1-\Pi(q,\Omega_m)/\gamma$ vs Ω_m at different q in a finite square lattice of size $L=20a$ (solid lines) and an infinite system (dashed lines). For the finite system there is a large intermediate region (dotted ellipse), where the slope of Π appears roughly independent of q. Panel (b) – the frequency variation of $\delta\Pi=\Pi(q,\Omega_m)-\Pi(q,0)$ in our model vs QMC data from Ref. [17] (up to a constant shift [27]). Panel (c) – phenomenological form of $\delta\Pi(q,\Omega_m)$, Eq. (2), vs QMC data [27].

fermionic states is the reduction (and eventual cutoff) of phase space for excitations. This is because terraces that are parallel to $\mathbf{q}$ get longer and longer as $\cos\theta\to 0$. We account for this effect by replacing the fermions with a liquid, keeping just the gap of width q_1 around the Fermi surface (Fig. 1). Our approximation keeps the essential physics of the cutoff but ignores further strong discreteness-based behavior occuring for $\beta\sim 1$. Then, if we restrict our attention to states near the Fermi surface, we can rewrite the interaction as:

$$H_I\propto\sum_{\mathbf{q}}\int d\theta d\epsilon_k\ f(\theta)\phi_{\mathbf{q}}\psi^\dagger_{\mathbf{k}(\theta)-\frac{\mathbf{q}}{2}}\psi_{\mathbf{k}(\theta)+\frac{\mathbf{q}}{2}}\Phi(\mathbf{q},\epsilon_k,\theta). \tag{7}$$

Here, $\epsilon_k=v_F(k-k_F)$ measures the distance from the FS and $f(\theta)$ is the form-factor at the FS. We separate the effects due to order parameter non-conservation from finite-size effects, and focus on the latter, by setting $f(\theta)=1$ (for $f(\theta)=1$ the order parameter *is* conserved). The function Φ is an indicator function due to finite size of a system. It accounts for the lack of $k-$states in an annulus of width q_1 around the FS (see Fig. 1 for visualization),

$$\Phi(\mathbf{q},\epsilon_k,\theta)=\Theta(|2\epsilon_k+\mathbf{v_F}(\theta)\cdot\mathbf{q}|-v_Fq_1)\times \Theta(|2\epsilon_k-\mathbf{v_F}(\theta)\cdot\mathbf{q}|-v_Fq_1), \tag{8}$$

Within the model, for β close to one, the suppression effect is proportional to $(1-\beta)^{3/2}$. To see this, note that as we move around the FS, the available phase space for particle-hole excitations is $\mathbf{v_F}\cdot\mathbf{q}-v_Fq_1=v_Fq(\cos\theta-\beta)$. Because of this restriction, the polarization bubble is proportional to

$$\int_0^{\theta_\beta}d\theta\ (\cos\theta-\beta)\sim(1-\beta)^{3/2},\quad \theta_\beta=\cos^{-1}\beta, \tag{9}$$

(we used $\theta_\beta\sim(1-\beta)^{1/2}$ for $1-\beta\ll 1$). This is the reasoning behind Eq. (2).

In addition to the damping term, the polarization bubble has a static piece, which renormalizes the bosonic mass and shifts the position of the QCP. This last term also gets modified in a finite system in such a way that the bosonic mass remains positive at a QCP of an infinite system, i.e., finite-size effects shift the system *away* from the critical point. This finite bosonic mass affects the self energy. In an infinite system $\Sigma(\mathbf{q},\omega)\sim\omega^{2/3}$ displays a non-FL behavior at a QCP. In a finite-size system, the mass term protects the FL behavior at low frequencies, which is the content of Eq. (3).

We demonstrate this behavior by explicitly calculating the polarization bubble and the self energy for the approximate model of Eqs. (4)-(8). We assume a parabolic dispersion and calculate the one-loop diagrams. To calculate the one-loop polarization bubble at $T\to 0$ we take into account only those $k-$ states that are on opposite sides of the boundary of the Fermi surface. In this case the indicator function can be recast as

$$\Phi=\Theta\left(|\mathbf{v_F}(\theta)\cdot\mathbf{q}|-v_Fq_1\right)\times \Theta\left(\mathbf{v_F}(\theta)\cdot\mathbf{q}-v_Fq_1-|2\epsilon_k|\right) \tag{10}$$

The polarization is then given by:

$$\Pi(\mathbf{q},\Omega)=\frac{m_0g^2\chi_0}{\pi^2}\int_0^{\theta_\beta}\frac{(\cos\theta-\beta)\cos\theta}{\alpha^2+\cos^2\theta}\,d\theta. \tag{11}$$

where m_0 is the bare fermionic mass. The limits of the integration are precisely those defined by the finite size effect of Eq. (10). Evaluating the integrals we find

$$\Pi(\alpha,\beta)=\frac{2\gamma}{\pi}\left[\cos^{-1}\beta-\frac{\alpha}{(1+\alpha^2)^{1/2}}\left(\tan^{-1}\frac{\alpha}{\beta}\frac{(1-\beta^2)^{1/2}}{(1+\alpha^2)^{1/2}}+\frac{\beta}{\alpha}\tanh^{-1}\frac{(1-\beta^2)^{1/2}}{(1+\alpha^2)^{1/2}}\right)\right] \quad (12)$$

where $\gamma=m_0g^2\chi_0/2\pi$. One can easily check that $\Pi(\alpha,\beta)$ vanishes at $\alpha\to\infty$ and at $\beta=1$. When $\beta\ll\alpha\ll1$, $\Pi(\alpha,\beta)\approx\gamma\,(1-\beta\log 2/\alpha-\alpha)$ Near $\beta=1$, $\Pi(\alpha,\beta)\approx 1.2\gamma(1-\beta)^{3/2}/(1+\alpha^2)$.

We next calculate the fermionic self-energy

$$\Sigma(\mathbf{k},\omega_m)=g^2\int\frac{d\Omega d^2q}{(2\pi)^3}\frac{\tilde{\chi}(\mathbf{q},\Omega_m)}{i(\omega_m+\Omega_m)-\mathbf{v_F}\cdot\mathbf{q}}, \quad (13)$$

where $\tilde{\chi}^{-1}=\chi^{-1}+\Pi$. An evaluation of Eq. (13) at $m=0$, $\beta\ll\alpha\ll1$ (i.e. large systems and low frequencies) yields

$$i\Sigma(\omega_m)=\frac{1}{\sqrt{3}}\left(\frac{\gamma}{v_F}\right)^{2/3}(v_Fq_1\log\alpha_L)^{2/3}\times \times\left[\left(1+\frac{\omega_m}{v_Fq_1\log\alpha_L}\right)^{2/3}-1\right], \quad (14)$$

where

$$\log\alpha_L=\frac{4}{3}\log\frac{v_Fq_L}{\omega_m},\quad q_L=(8\gamma q_1^2)^{1/4}. \quad (15)$$

Eq. (14) is the explicit version of Eq. (3). We plot $\Sigma(\omega_m)$ along with QC and FL asymptotics ($\omega^{2/3}$ and ω, respectively) in Fig. 3a. We see that in a finite-size system $\Sigma(\omega_m)$ preserves a FL form up to large ω_m/v_Fq_1.

An additional popular probe in QMC is the Green's function on the Fermi surface along the imaginary time axis [25],

$$G(\tau,\mathbf{v_F})=T\sum_{\omega_n}\frac{e^{i\omega_n\tau}}{i\omega_n-\Sigma(\omega_n)} \quad (16)$$

In a FL, $G(\tau=1/2T)=Z_{qp}/2$. For $\Sigma\sim\omega_n^{2/3}$ $G(\tau=T/2)=T^{1/3}$, indicating that the quasiparticle residue vanishes at $T=0$ (the actual power is $T^{1/2}$ due to special form of the self-energy at the first Matsubara frequency [26]). Because the sum is dominated by the terms with $n=O(1)$, the finite size behavior of Σ is important. Plugging parameters extracted from the data of Ref. [17] into Eq. (14) and substituting into Eq. (16), we obtain Z_{qp}, which decreases as a function of T, but still approaches a finite value at $T\to0$ (see Fig. 3b). In this limit, our calculation yields $Z_{qp}=0.76$. Ref. [17] found a very similar $Z_{qp}=0.75-0.85$ in the low temperature regime [27].

Discussion. We showed that finite size effects modify the low energy properties of the particle-hole polarization bubble and the fermionic self energy near a $q=0$ QCP. We found three effects: i) the slope of the frequency dependence of $\Pi(q,\Omega_m)$ changes from its universal $1/q$ form to almost $q-$independent, ii) the bosonic mass gets a q dependent correction; iii) the non-analyticity of the electronic self energy is cut off below a certain frequency. In a real finite-size system the strength of (i) and (ii) is actually a bit smaller than in our model, where the polarization appears to vanish at $q=q_1$ for all Ω_m. In practice, there will always be a residual polarisation coming from a) broadening due to finite self energy, and b) the irregularity of the separation between filled/empty states due to a discrete structure of the FS in a finite system. Both these features can be seen just by studying the left panel of Fig. 1. A translational symmetry breaking inherent in any finite system also induces broadening. Nevertheless we do capture the main features observed in QMC studies.

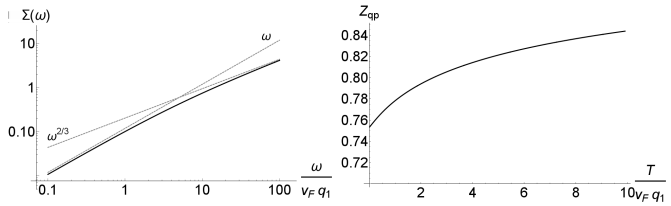

(a) (b)

FIG. 3. Self energy of a finite system. In an infinite system the self energy has a non-analytic behavior at low temperatures, $\Sigma(\omega)\sim\omega^{2/3}$. In a finite system the nonanalytic behavior is cut off at a scale of $\omega\sim v_Fq_1$. The left panel depicts $\Sigma(\omega)$ for a system of size $L=20a$. The dashed grey lines are guides to the eye of $\omega,\omega^{2/3}$. Note how the FL type behavior extends over a numerically large region near v_Fq_1. The right panel depicts the quasiparticle residue as obtained from Eq. (16) [27].

Our results may be considered a variant of the well-known "closed-shell" problem, where finite sizes introduce gaps in the (discrete) density of states $n(\omega)$ at fractional fillings [28]. These gaps affect low energy physics such as transport [29]. It is possible to reduce such gap effects by inserting a small magnetic field [30] as was done in [17]. However, as long as the fermions are truly itinerant, the discreteness of $\mathbf{k}$ will not be removed. Our results' agreement with the numerical data in [17] indicate that such effects persist even with some lattice symmetry breaking and significant coupling.

We thank E. Berg, S. Lederer, S. Kivelson, Y. Schattner, D. Chowdhury, R. Fernandes, X. Wang and S. K. Srivastava for useful discussions. This work was supported by the NSF DMR-1523036.

* ayklein@umn.edu

[1] H. V. Lohneysen, A. Rosch, M. Vojta, and P. Wolfle, Rev. Mod. Phys. 79, 1015 (2007).

[2] E. Fradkin, S. A. Kivelson, M. J. Lawler, J. P. Eisenstein, and A. P. MacKenzie, Annual Review of Condensed Matter Physics 1, 153 (2010) ArXiv:0910.4166.

[3] P. A. Lee, Phys. Rev. Lett. 63, 680 (1989); B. Blok and H. Monien, Phys. Rev. B 47, 3454 (1993); V. Oganesyan, S. A. Kivelson and E. Fradkin, Phys. Rev. B 64, 195109 (2001); W. Metzner, D. Rohe and S. Andergassen, Phys. Rev. Lett. 91, 066402 (2003).

[4] B. L. Altshuler, L. B. Ioffe, and A. J. Millis, Phys. Rev. B **50**, 14048 (1994).

[5] C. Nayak and F. Wilczek, Nuclear Physics B 430, 534 (1994).

[6] A. J. Millis, Phys. Rev. B 45, 13047 (1992).

[7] Ar. Abanov, A.V. Chubukov, and J. Schmalian, Adv. Phys. 52, 119 (2003); Ar. Abanov and A.V. Chubukov, Phys. Rev. Lett., 93, 255702 (2004).

[8] S. A. Hartnoll, R. Mahajan, M. Punk, and S. Sachdev, Phys. Rev. B 89, 155130 (2014); A. A. Patel, P. Strack, and S. Sachdev, Phys. Rev. B 92, 165105 (2015).

[9] T. Senthil, Phys. Rev. B 78, 035103 (2008).

[10] M. A. Metlitski and S. Sachdev, Phys. Rev. B **82**, 075128 (2010).

[11] S.-S. Lee, Phys. Rev. B **80**, 165102 (2009).

[12] M. A. Metlitski and S. Sachdev, Phys. Rev. B **82**, 075127 (2010).

[13] D. F. Mross, J. McGreevy, H. Liu, and T. Senthil, Physical Review B 82, 045121 (2010).

[14] T. Holder and W. Metzner, Phys. Rev. B 92, 245128 (2015).

[15] I. Mandal, Phys. Rev. B 94, 115138 (2016).

[16] A. Eberlein, I. Mandal, and S. Sachdev Phys. Rev. B 94, 045133 (2016) and references therein.

[17] Y. Schattner, S. Lederer, S. A. Kivelson, and E. Berg, Phys. Rev. X **6**, 031028 (2016).

[18] D. L. Maslov and A. V. Chubukov Phys. Rev. B 81, 045110 (2010).

[19] We leave proof of this statement to a future publication.

[20] L. Dell'Anna and W. Metzner, Phys. Rev. B **73**, 045127 (2006).

[21] M. Punk, Phys. Rev. B **94**, 195113 (2016).

[22] A. D. Huxley, S. Raymond, and E. Ressouche, Phys. Rev. Lett. **91**, 207201 (2003).

[23] C. Stock, D. A. Sokolov, P. Bourges, P. H. Tobash, K. Gofryk, F. Ronning, E. D. Bauer, K. C. Rule, and A. D. Huxley, Phys. Rev. Lett. **107**, 187202 (2011).

[24] A. V. Chubukov, J. J. Betouras, and D. V. Efremov, Phys. Rev. Lett. **112**, 037202 (2014).

[25] N. Trivedi and M. Randeria, Phys. Rev. Lett. **75**, 312 (1995).

[26] A. V. Chubukov and D. L. Maslov, Phys. Rev. B **86**, 155136 (2012).

[27] In order to compare our analytic expressions in Eqs. (4), (12), (14) with the QMC data, we used the average value of the Fermi vector and velocity k_F, v_F for a cubic lattice. We extracted the value of γ by comparing the values of $\Pi(0,0)$ at $g = 0$ and finite g. We extracted c^2 by fitting the data for $q = 0$ to a quadratic form. The value of χ_0 was taken from Ref. [17]. Finally, the constant shift and global γ used in the analytic lines of Fig. 2b were found using a best fit to the raw data, so as to be self consistent; so was the slope in Fig. 2c. However, using the value of γ we extracted from [17] gives an equally good fit.

[28] R. R. d. Santos, Brazilian Journal of Physics **33**, 36 (2003).

[29] R. Mondaini, K. Bouadim, T. Paiva, and R. R. dos Santos, Phys. Rev. B **85**, 125127 (2012).

[30] F. F. Assaad, Phys. Rev. B **65**, 115104 (2002).